Journal of Power Sources 252 (2014) 8–13

Contents lists available at ScienceDirect

Journal of Power Sources

journal homepage: www.elsevier.com/locate/jpowsour

Short communication

Internal resistance matching for parallel-connected lithium-ion cells and impacts on battery pack cycle life

Radu Gogoana [a], Matthew B. Pinson [b,*], Martin Z. Bazant [c,d], Sanjay E. Sarma [a]

[a] Department of Mechanical Engineering, Massachusetts Institute of Technology, 77 Massachusetts Avenue, Cambridge, MA 02139, USA
[b] Department of Physics, Massachusetts Institute of Technology, 77 Massachusetts Avenue, Cambridge, MA 02139, USA
[c] Department of Chemical Engineering, Massachusetts Institute of Technology, 77 Massachusetts Avenue, Cambridge, MA 02139, USA
[d] Department of Mathematics, Massachusetts Institute of Technology, 77 Massachusetts Avenue, Cambridge, MA 02139, USA

HIGHLIGHTS

- We demonstrate the importance of resistance matching in battery packs.
- At 4.5C charge and discharge, 20% resistance mismatch reduces lifetime by 40%.
- We quantitatively explain experimental results using a model of SEI formation.
- Resistance mismatch causes uneven current sharing.
- Uneven current results in high operating temperatures, decreasing lifetime.

GRAPHICAL ABSTRACT

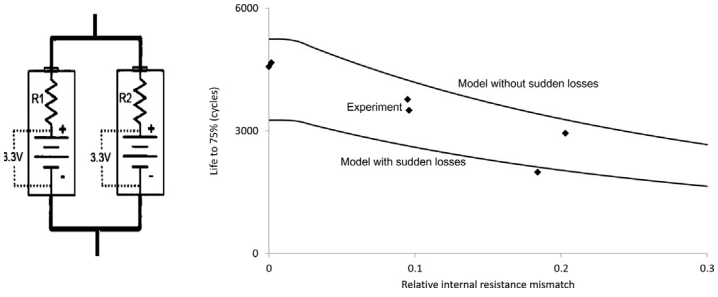

ARTICLE INFO

Article history:
Received 3 July 2013
Received in revised form
25 November 2013
Accepted 26 November 2013
Available online 10 December 2013

Keywords:
Lithium
Battery
Pack
Lifetime
Resistance
Temperature

ABSTRACT

When assembling lithium-ion cells into functional battery packs, it is common to connect multiple cells in parallel. Here we present experimental and modeling results demonstrating that, when lithium ion cells are connected in parallel and cycled at high rate, matching of internal resistance is important in ensuring long cycle life of the battery pack. Specifically, a 20% difference in cell internal resistance between two cells cycled in parallel can lead to approximately 40% reduction in cycle life when compared to two cells parallel-connected with very similar internal resistance. We show that an internal resistance mismatch leads to high current into each cell during part of the charging cycle. Since capacity fading is strongly dependent on temperature, and hence on charging rate when this rate is sufficiently high, the high current leads to substantially accelerated capacity fade in both cells. A model, based on the formation of a solid-electrolyte interphase, is able to explain the dependence of lifetime on resistance mismatch, and also identifies the importance of random sudden capacity losses.

1. Introduction

In this paper, we present experimental results showing the impact of internal resistance mismatch on cycle life, and outline a model to explain this effect.

Internal resistance mismatch becomes an important problem for applications where the battery pack is subjected to high C rates, and required to have a long cycle life (many hundreds to tens of thousands of cycles). Example applications include hybrid vehicle and power tool battery packs.

The detrimental effect of internal resistance mismatch between parallel-connected cells arises because differences in internal resistance lead to uneven current distribution within the cells; the

* Corresponding author. Tel.: +1 617 253 3178; fax: +1 617 258 5766.
E-mail address: mpinson@mit.edu (M.B. Pinson).

0378-7753/$ – see front matter © 2013 Elsevier B.V. All rights reserved.
http://dx.doi.org/10.1016/j.jpowsour.2013.11.101

List of symbols

A	surface area on which solid-electrolyte interphase (SEI) can form, m^2
c	concentration of S at the graphite surface, M
D	diffusivity of S through SEI, $m^2\ s^{-1}$
D_0	diffusivity of S through SEI when charging current is negligible, $m^2\ s^{-1}$
E	activation energy for the diffusion of S through SEI, J
I	maximum charging C rate to which a cell is subjected in a particular cycle
k	rate constant of the reaction forming SEI, $s^{-1}\ m^{-2}\ M^{-1}$
m	molecular mass of SEI, kg
Q	capacity of a cell, Ah
Q_0	capacity of a cell when uncycled, Ah
Q_1	capacity of the more resistive cell in a cell group, Ah
Q_2	capacity of the less resistive cell in a cell group, Ah
Q_x	excess capacity of the more resistive cell in a cell group, Ah
R_1	resistance of the more resistive cell in a cell group, Ω
R_2	resistance of the less resistive cell in a cell group, Ω
S	the species that reacts with Li to form SEI
s	thickness of the SEI, m
T	temperature, K
t	time, s
α	parameter quantifying the dependence of D on current
Δ	internal resistance mismatch
ρ	density of SEI, $kg\ m^{-3}$

resulting unexpectedly high currents decrease battery pack life. Current distribution within parallel-connected cells is typically not monitored in commercial battery packs in order to reduce battery management system complexity and cost. This means that the effect of internal resistance mismatch must be quantified in order to assess the importance of this consideration in battery pack assembly.

In this paper we quantify the relationship between internal resistance mismatch and battery degradation, combining experimental data with a simple model of capacity fade. This model assumes that the growth of a solid electrolyte interphase is the primary cause of capacity fade [1,2], though the conclusions regarding the importance of internal resistance mismatch do not rely on the details of the fade mechanism.

2. Experimental setup

2.1. Cell characterization

The cells used in this study were commercially available 2.2 Ah cylindrical $LiFePO_4$ cathode, graphite anode cells, designed for use in high-C-rate applications.

The internal resistance of 72 cells was tested. Internal resistance was measured at 50% state of charge (SOC) with a 15 s DC pulse of 40 A (17C). While there is no commonly accepted standard for measuring the internal resistance of lithium-ion batteries, we chose this current and time profile because it is relevant to the duty cycle seen by these cells in hybrid vehicles and power tools. A comparison of several methods for the internal resistance of lithium-ion cells is provided by Schweiger et al. [3]. The 15 s current pulse allows the effects of the mass-transfer limited reaction to show. Longer delay times can lead to significant self-heating of the cell which affects the measured internal resistance. This 17C discharge rate is within the specified rating for this high-power cell, of 32C continuous discharge and 55C for 10-s peaks. The characterization tests were done on bare cells in a background room temperature of 25 °C.

The resistance difference between the most and least resistive cells was 24.7%. The maximum difference in capacity in this same batch of cells (one full discharge cycle at 17C continuous discharge current) was 3.6%. For the purposes of this experiment, the differences in initial capacity were considered to be negligible compared to the differences in internal resistance (Fig. 1).

2.2. Lifetime cycling setup

Six battery packs (each containing two cells connected in parallel, as depicted in Fig. 5) were tested using the method described below. For further reference within this paper, two parallel-connected cells are called a “cell group”. The current to each cell and the temperature of each cell were recorded. A photo of the experimental cell groups is seen in Fig. 2. The cell group assembly was designed to thermally decouple the two cells: each cell had its own 8 cm wire lead and the cells were physically separated with plastic spacers so that the casings were 8 mm apart.

The cycling tests were carried out with the following parameters:

- Constant current charging of 20A to 3.65 V per cell group (4.5C)
- Constant voltage held at 3.65 V with termination current of 1 A
- 1 min rest period between charge and discharge
- Constant current discharge of 20 A to 2.40 V (4.5C)
- 1 min rest period between discharge and charge.

Cycling tests were done at a loosely controlled background room temperature that varied between 24 °C and 31 °C, and the temperature of each cell’s aluminum casing was monitored continuously. The background temperature profile was the same for all cells. Data collection was done using an Agilent 34980A multifunction switch/measure mainframe with a 34921A multiplexer card. Charging, discharging and current control automation was done using 6 FMA Direct PowerLab 6 bidirectional chargers, running on a regulated 24 V DC bus.

3. Results

Fig. 3 plots cycle life, defined as the number of cycles for the cell group to reach 75% of the initial capacity, vs. internal resistance mismatch, defined by

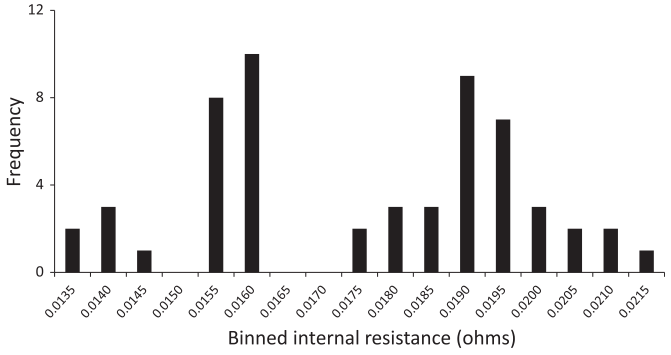

Fig. 1. Internal resistance distribution of cells tested.

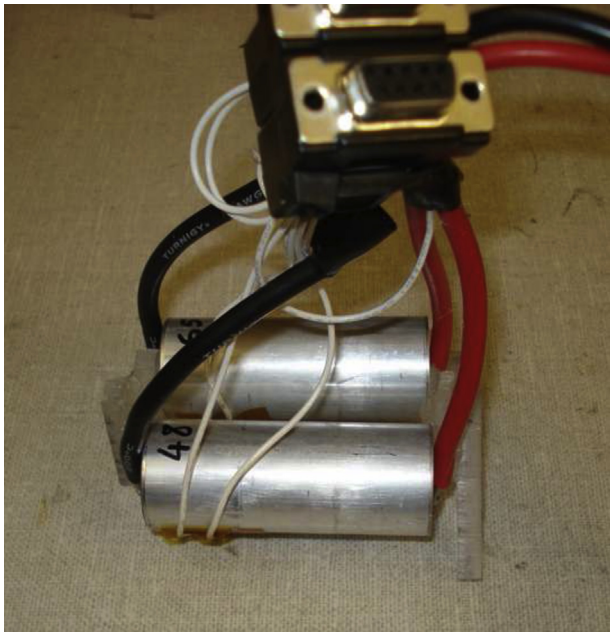

Fig. 2. Lifetime cycling setup.

$$\Delta = \frac{R_1 - R_2}{R_2}, \quad (1)$$

where R_1 is the resistance of the more resistive cell and R_2 that of the less resistive. The data show that higher internal resistance mismatch results in shorter lifetime.

In order to show that the *difference* in internal resistance between cells in a parallel-connected group determines lifetime, and not the initial resistance of the individual cells, cell lifetime is plotted against the initial resistance of each cell in Fig. 4. There is no clear dependence of lifetime on the internal resistance of an individual cell: in particular, considering all cells together and grouping cells according to internal resistance difference would give opposite signs of such dependence. Thus, if the internal resistance of an individual cell has any effect on lifetime, it is much smaller than the effect of the internal resistance mismatch between cells connected in parallel. Of course, such an effect might be of scientific interest and could be studied further, but the larger effect is of more engineering importance.

4. Discussion

Previous work [1,4] has identified the growth of the solid-electrolyte interphase layer (SEI) on the graphite particles in the negative electrode as the primary mechanism of capacity fade in lithium ion batteries subjected to typical cycling conditions. After the first few cycles, SEI growth is limited by the rate at which reacting molecules from the electrolyte are transported through the existing SEI to the graphite surface, at which they react with lithium to form SEI. Experimental results show that the capacity fade rate does not strongly depend on current, provided that the current is small, but increasing temperature greatly hastens capacity fade [5,6]. In the case of the cells that we tested, the 4.5C charge and discharge currents were large enough to impact the capacity fade rate, likely by increasing the cells' operating temperature.

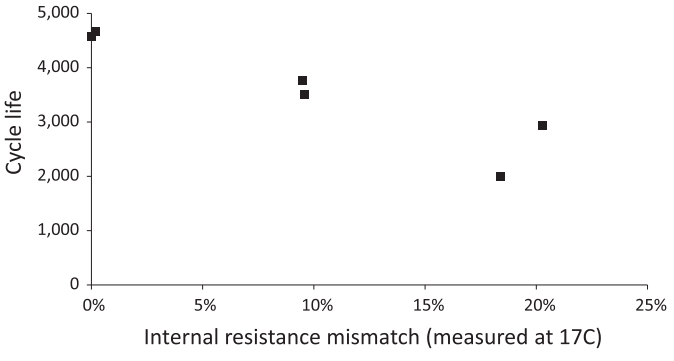

Fig. 3. Cycle life vs. initial resistance mismatch, showing lower cycle life at higher mismatch.

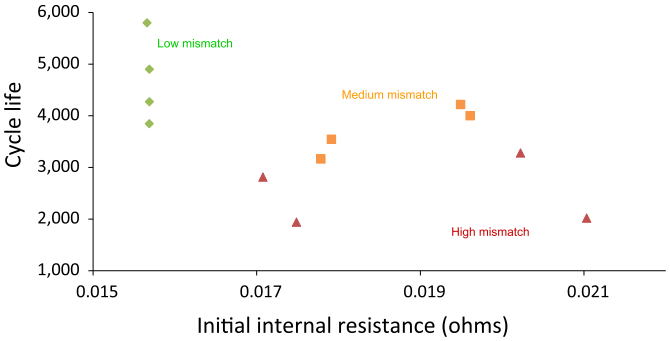

Fig. 4. Cycle life vs. initial resistance, showing little dependence of cycle life on an individual cell's initial resistance.

When two cells with different internal resistance are charged in parallel, the current experienced by each cell is not constant. Early in the charging process, the less resistive cell experiences a higher current. This may cause it to approach a fully charged state sooner than the more resistive cell, resulting in an increase in current to the more resistive cell towards the end of charging. A large difference in internal resistance thus results in high maximum charging current to both cells in the cell group, which is shown in Fig. 6. The less resistive cell 2 has higher current early in discharge and charge; the later increase in current to cell 1 is more apparent on discharge than on charge.

It is important to note that the shape of the current distribution curve in Fig. 4 is linked to shape of the voltage vs. capacity curve of

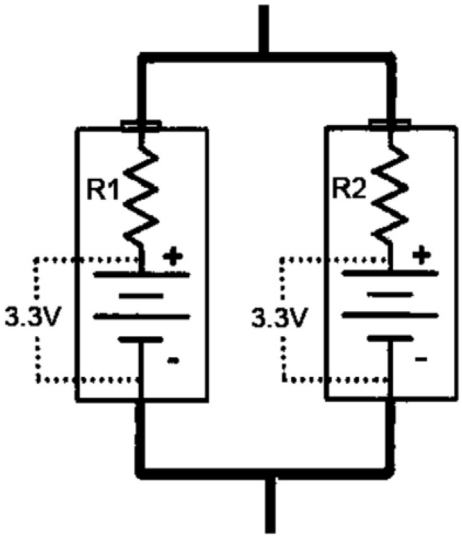

Fig. 5. A circuit diagram of the cell group arrangement tested in this work.

$LiFePO_4$ cells, which is relatively flat between approximately 10% and 90% SOC. For other Li-ion cell chemistries that have more sloped voltage vs. capacity curves ($LiMn_2O_4$, $LiCoO_2$, etc), we expect a "balancing-out" effect to occur throughout the charge and discharge cycles. We only tested $LiFePO_4$ cells. Because capacity and voltage are more closely related for those chemistries, we expect that both cells in a parallel-connected configuration will reach end-of-discharge more evenly without a large difference in current between the two cells toward the end of the cycle.

The experimental results presented here show that a higher maximum current increases the capacity fade rate, even when average current is fixed. This could arise because resistive heating causes an increase in temperature, which exponentially increases the rate of capacity fade [1]. Although the temperature of all cells increased during cycling, there was no significant correlation between the temperature of an individual cell and either current or the rate of capacity fade. Thus, if the dependence of capacity fading on current is due to a temperature increase, this temperature increase must be highly localized inside the cell. Alternatively, the accelerating effect of very high current on capacity fade may be separate from any temperature effect.

The difference in temperature between individual cells within a cell group remained low. For example, a 11% difference in current led to a 0.7 °C difference in temperature between cells. The temperature difference within the cells was most likely localized near the center of the spiral-wound electrode, which was difficult to measure practically in our experiment. Only the temperature of the cell casing, which was exposed to cooling airflow, was measured. The impact of temperature on the cycle life of lithium-ion cells has been studied by several groups [1,2,7,8].

5. Analysis

5.1. Dependence of fade rate on current

Two of the present authors presented a model of capacity fade that shows good agreement with experimental results [4]. According to this model, capacity fade is due to the formation of a gradually thickening SEI on the surface of graphite particles: the thickness s of this SEI layer is described by the differential equation

$$\frac{ds}{dt} = \frac{kcDm}{\rho(D+ks)}. \tag{2}$$

Here k is the rate constant of the reaction forming SEI, m is the molecular mass and ρ the density of the SEI formed, c is the concentration in the electrolyte of the species that reacts with lithium to form SEI and D is the diffusivity of this species through the SEI. The capacity loss is proportional to SEI thickness, so

$$\frac{dQ}{dt} = -\frac{kcDA^2\rho}{\rho DA + km(Q_0 - Q)}, \tag{3}$$

where Q is the remaining capacity, Q_0 is the initial capacity and A is the surface area on which SEI can form [4].

This model requires the hypothesis of a particular dependence of D on C rate. It has been convincingly shown that D depends strongly on temperature: an Arrhenius dependence,

$$D \propto \exp\left(-\frac{E}{k_B T}\right), \tag{4}$$

is consistent with experimental data [4]. Assuming that the cell temperature is elevated above room temperature by an amount proportional to the C rate, and that this elevation is much smaller than room temperature, which is itself much smaller than E/k_B, equation (4) can be expressed as

$$D = D_0 \exp(\alpha I), \tag{5}$$

where I is the C rate and α is a constant. Combining this with an assumption that any dependence of k on C rate was unimportant, we used equation (3) to model capacity fade in all of the cells. A least squares fit to the experimental data was used to calculate values of the parameters D_0, α and k. The value of D as a function of C rate is shown in Fig. 7. The model was sufficient to describe capacity fade until 75% capacity for most of the cells studied. One cell showed anomalously slow capacity fade and was excluded from the analysis, as including it caused the calculated fade rate of other cells to differ from the obvious cluster.

Fig. 8 compares experimental capacity fade with the model prediction for the two cells with smallest and largest error.

Using this model of capacity fade, lifetime to 75% of total capacity can be predicted for a pair of cells with arbitrary difference in internal resistance. This prediction relies on the assignment of a maximum charging current to each cell at each cycle. For the cell with lower resistance, this can be calculated assuming that the ratio of resistances does not change with degradation.

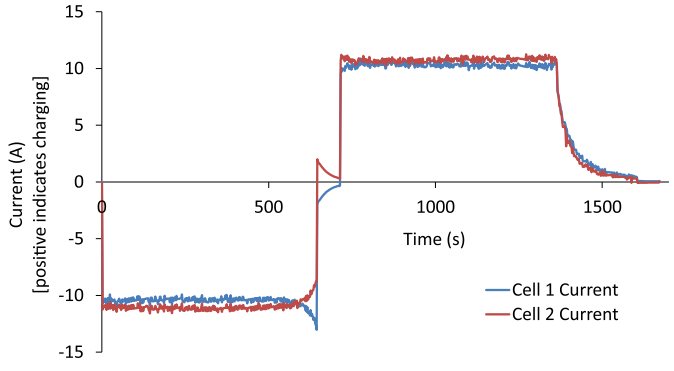

Fig. 6. Current distribution within two parallel-connected cells upon cycling (initial resistance difference of 18%).

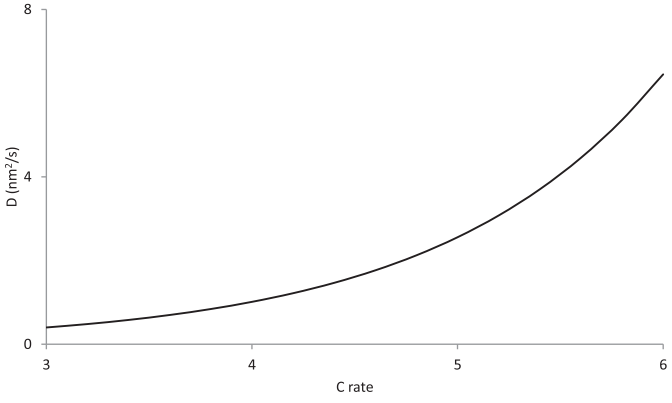

Fig. 7. D as a function of C rate, fit to measured capacity fade.

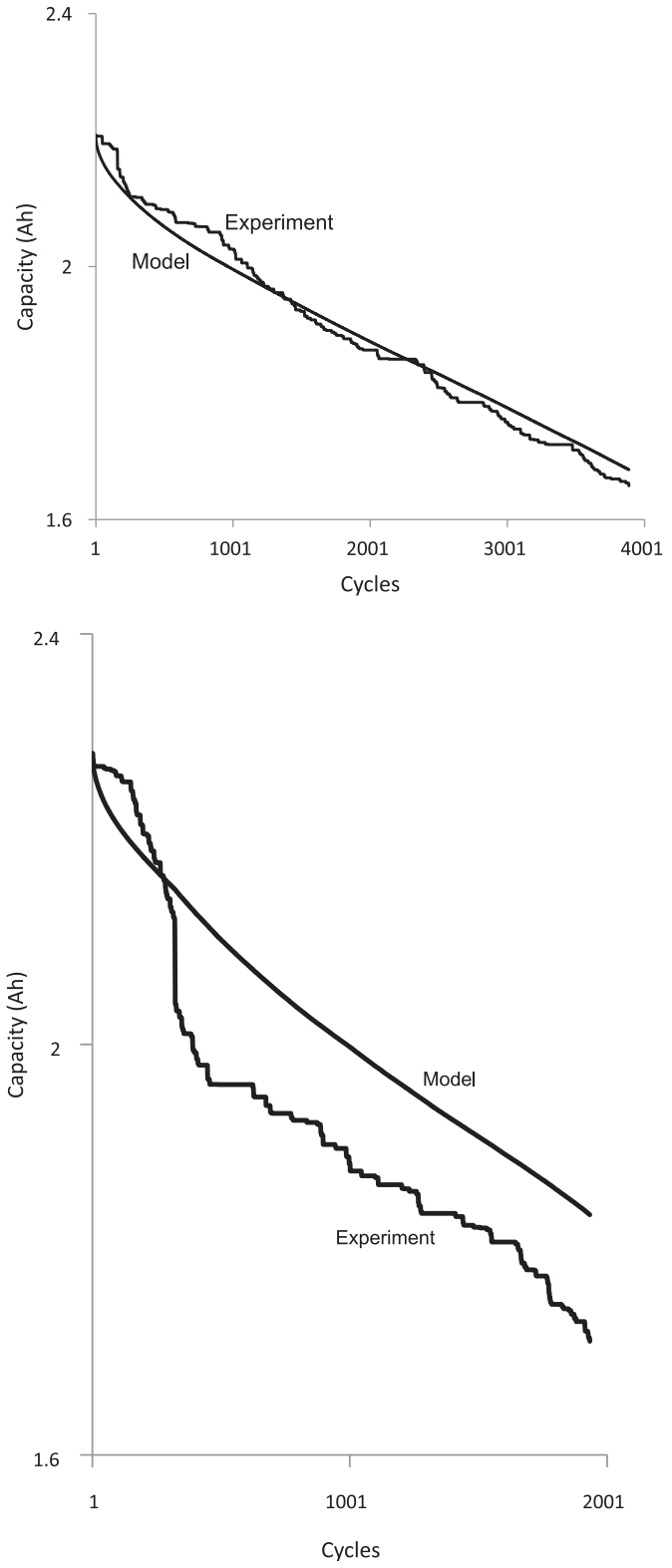

Fig. 8. Experimental and model capacity fade for two cells.

The maximum charging current to the cell with higher resistance will come at the end of charging, when the other cell nears a fully-charged state. It was observed that the maximum charging current measured experimentally for the more resistive cell in a pair was linearly related to the "excess capacity" Q_x, defined by

$$Q_x = Q_1 - \frac{Q_2 R_2}{R_1} \tag{6}$$

where Q_1 and R_1 are the capacity and resistance of the more resistive cell and Q_2 and R_2 the capacity and resistance of the less resistive cell. The excess capacity is thus the charging capacity remaining in the more resistive cell when the less resistive cell has finished charging, assuming that the charging rates remain constant. The observed linear relationship, shown in Fig. 9, was used as an input into the model-based prediction.

This increase in maximum charging current from 9.5 A to 12 A (4.3C–5.5C) can be a significant factor in the capacity fading of the cell. Observed data by Wang et al. [6] on the same $LiFePO_4$ cells that we tested, showed an exponential increase in capacity fade with C-rate. The curve-fitted model that they obtained from their experimental data is shown in Fig. 10. Although they only tested the impact of higher discharge currents (their charge current in testing was a constant 2C), it is possible that a similar relationship exists on charging C-rate, and that the jump from 4.3C to 5.5C on charging was responsible for this difference in capacity fade.

Previous work [4] has presented a model that explains experimental data with a degradation rate that is independent of current. In fact, since the model identifies time rather than charge throughput as the determinant of capacity fade, cells exposed to higher C rates are expected to have a longer cycle life. The model does display a strong dependence of degradation rate on temperature, and it is likely that the importance of fast charging is that it increases temperature through resistive heating within the cell. In the experiments presented here, there was no apparent relationship between the measured temperature at the outside of the cell and fade rate, so if heating is indeed the cause of increased capacity fade, it must be somewhat localized within the spiral-wound electrode. This localized temperature rise can be estimated by comparing the change in the rate of capacity fade due to a C-rate increase, with that due to an increase in ambient air temperature. According to the SEI formation model [4], a 10 °C increase in temperature increases the capacity fade rate by approximately 40%, due to a doubling of the diffusivity of electrolyte molecules through the SEI. The same increases were found in the model applied to the present work, when maximum charging current was increased by 0.7C. In other words, a 10 °C increase in background temperature or a 0.7C increase in maximum charging rate apply approximately equal stress to the battery in terms of capacity fade rate.

5.2. Lifetime prediction

Fig. 11 shows the predicted lifetime as a function of relative resistance difference, calculated by combining equations (3), (5) and (6) with the empirical relationship shown in Fig. 9. The top curve accounts only for gradual capacity fade due to SEI formation. In addition, many cells experienced a sudden capacity loss of up to 100 mAh towards the beginning of the cycling process. These capacity losses could result from isolation of active material from the conductive matrix, due to SEI growth or physical separation. The bottom curve represents a worst-case scenario, where both cells experience a 100 mAh capacity loss at the beginning of cycling, followed by gradual SEI formation. The model explains the observed decrease of lifetime with an increase in internal resistance mismatch, and that the observed scatter is due to random sudden capacity losses. These random losses can drastically reduce cycle life, and so are important to monitor (and ideally prevent), even though on average most capacity fade is due to gradual SEI formation.

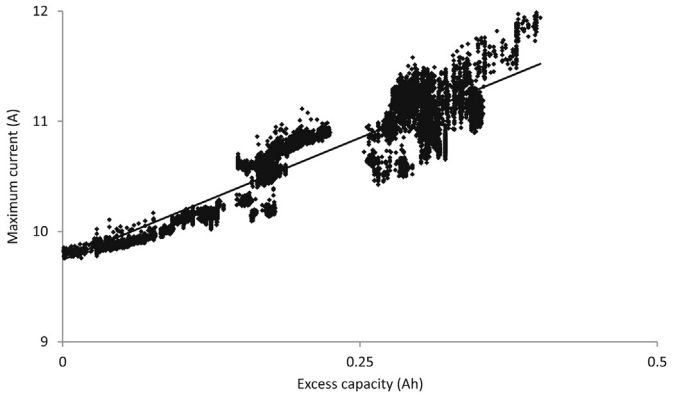

Fig. 9. Maximum charging current to the more resistive cell as a function of the excess capacity of this cell (defined by equation (6)). More capacity remaining in one cell at the end of a charge cycle leads to higher maximum charge current to that cell.

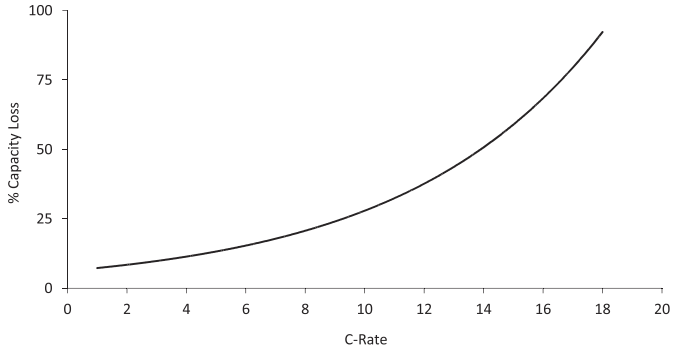

Fig. 10. Modeled capacity fade as a function of C rate according to Wang et al. [6].

The modeling described in this paper could be applied to any situation where cells are charged at a C rate high enough to increase temperature. In order to obtain a prediction of lifetime, it is vital to know the actual C rate to which a cell is exposed. For instance, if more than two cells are connected in parallel, the extra current imposed when one cell reaches capacity will be shared between the others, and a detailed measurement or model of this sharing is necessary to allow a quantitative prediction of pack lifetime.

6. Conclusions and outlook

Mismatching of internal resistance in parallel-connected cells can lead to the more resistive cell taking a higher current toward the end of the discharge cycle. This can lead to premature aging if the cell is not designed to handle this abnormally high current. This work showed that this impact of resistance mismatch on battery life was substantially more important than any effect of single cell resistance.

Sorting and binning by internal resistance is beneficial for pack assemblers to better control the charge/discharge profiles that their cells will experience, reducing the probability of exposure to very high C rates and thus increasing average battery life.

There are two obvious areas where further experiments would be very valuable. First, this work examined only one circuit setup and cycling profile. Testing of a range of different setups would allow the assessment of the relevance of resistance mismatch in a variety of applications. For example, charging to less than full capacity would avoid the charge region in which current to the more resistive cell is greatest, and we expect that this would increase lifetime. Further experiments could test this hypothesis and whether it is sufficient to outweigh the underutilization of the cells.

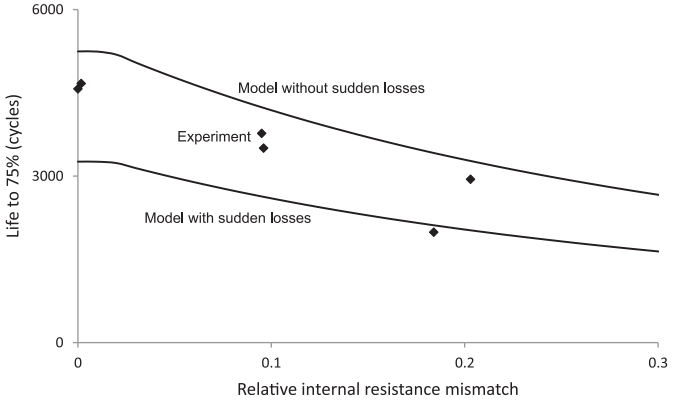

Fig. 11. Experimental and predicted lifetime as a function of internal resistance mismatch.

Second, the model presented here, and its agreement with experiment, suggest that the maximum charging current experienced by a cell has a strong impact on its degradation rate. A systematic study of cell degradation under carefully controlled charging current, with numerous identical cells subjected to a wide variety of charging profiles, would give very interesting fundamental information about the factors influencing degradation, as well as useful insight into the expected degradation of parallel-connected cells.

The understanding of how resistance mismatch leads to accelerated capacity fade, contributed by this work and potential future experiments, could be used to optimize manufacturing processes. Combining knowledge of how resistance mismatch affects lifetime with the intended application of the battery would make it possible to quantify the largest allowable tolerance windows for internal resistance. In turn, this can aid cost reductions in high-volume manufacturing, as well as in enabling the use of less sophisticated production equipment for low-volume manufacturing.

Acknowledgments

We thank Lennon Rodgers for useful comments on the manuscript.

References

[1] P. Arora, R.E. White, M. Doyle, J. Electrochem. Soc. 145 (10) (1998) 3647–3667.
[2] J. Vetter, P. Novák, M.R. Wagner, C. Veit, K.-C. Möller, J.O. Besenhard, M. Winter, M. Wohlfahrt-Mehrens, C. Vogler, A. Hammouche, J. Power Sources 147 (2005) 269–281, http://dx.doi.org/10.1016/j.jpowsour.2005.01.006. URL: http://linkinghub.elsevier.com/retrieve/pii/S0378775305000832.
[3] H.-G. Schweiger, O. Obeidi, O. Komesker, A. Raschke, M. Schiemann, C. Zehner, M. Gehnen, M. Keller, P. Birke, Sensors 10 (6) (2010) 5604–5625, http://dx.doi.org/10.3390/s100605604. URL: http://www.pubmedcentral.nih.gov/articlerender.fcgi?artid=3247723&tool=pmcentrez&rendertype=abstract.
[4] M.B. Pinson, M.Z. Bazant, J. Electrochem. Soc. 160 (2) (2013) A243–A250, http://dx.doi.org/10.1149/2.044302jes. URL: http://jes.ecsdl.org/cgi/doi/10.1149/2.044302jes.
[5] A.J. Smith, J.C. Burns, D. Xiong, J.R. Dahn, J. Electrochem. Soc. 158 (10) (2011) A1136, http://dx.doi.org/10.1149/1.3625232. URL: http://link.aip.org/link/JESOAN/v158/i10/pA1136/s1&Agg=doi.
[6] J. Wang, P. Liu, J. Hicks-Garner, E. Sherman, S. Soukiazian, M. Verbrugge, H. Tataria, J. Musser, P. Finamore, J. Power Sources 196 (8) (2011) 3942–3948, http://dx.doi.org/10.1016/j.jpowsour.2010.11.134. URL: http://linkinghub.elsevier.com/retrieve/pii/S0378775310021269.
[7] G.G. Botte, B.A. Johnson, R.E. White, J. Electrochem. Soc. 146 (3) (1999) 914–923. URL: http://jes.ecsdl.org/content/146/3/914.short.
[8] G. Ning, B.N. Popov, J. Electrochem. Soc. 151 (10) (2004) A1584–A1591, http://dx.doi.org/10.1149/1.1787631. URL: http://jes.ecsdl.org/cgi/doi/10.1149/1.1787631.